



Influence of biodiesel and diesel fuel blends on the injection rate and spray injection under cold conditions

Padipan Tinprabath, Camille Hespel, Somchai Chanchaona, Fabrice Foucher

► To cite this version:

Padipan Tinprabath, Camille Hespel, Somchai Chanchaona, Fabrice Foucher. Influence of biodiesel and diesel fuel blends on the injection rate and spray injection under cold conditions. ILASS – Europe 2014, 26th Annual Conference on Liquid Atomization and Spray System, Sep 2014, Bremen, Germany. hal-01077636

HAL Id: hal-01077636

<https://hal.science/hal-01077636>

Submitted on 26 Oct 2014

HAL is a multi-disciplinary open access archive for the deposit and dissemination of scientific research documents, whether they are published or not. The documents may come from teaching and research institutions in France or abroad, or from public or private research centers.

L'archive ouverte pluridisciplinaire **HAL**, est destinée au dépôt et à la diffusion de documents scientifiques de niveau recherche, publiés ou non, émanant des établissements d'enseignement et de recherche français ou étrangers, des laboratoires publics ou privés.

Influence of biodiesel and diesel fuel blends on the injection rate and spray injection under cold conditions

Padipan Tinprabath^{*1}, Camille Hespel¹, Somchai Chanchaona², Fabrice Foucher¹

¹PRISME, Université d'Orléans, France

²CERL, King Mongkut's University of Technology Thonburi, Thailand

^{*}Corresponding author: padipan.tinprabath@etu.univ-orleans.fr

Abstract

Fossil fuel supplies are decreasing every day due to excessive energy requirements. This problem can be solved by partly replacing fossil fuel with renewable biodiesel fuel. However, during the start-up of the engines under cold temperatures conditions can be different where biodiesel are used due to the low fuel injection pressure and the high cloud point and high pour point. It is consequently of interest to understand the behavior of the injector under cold conditions when operating with biodiesel and the impact on the combustion process. This article presents the experimental study of diesel fuel and biodiesel blends on injection flow. Bosch CRI 3.1 piezoelectric injection was used. The injectors are used on present diesel engine. Five fuels were tested: diesel fuel winter diesel fuel, two diesel-biodiesel blends: B20, B50, and pure biodiesel (B100). Injection pressures were set at 30-60 MPa for the study of the injection flow characteristics in room temperature, non-vaporizing conditions and cold conditions. Under cold temperature (268 K and 265 K), the experimental results show that not effect of the injection delay all fuels, the delay closing in the fuel of injection increases with the biodiesel content, B100 fuel showing the most delayed closing, at cold temperature the discharge coefficient for all fuels is lower than at room temperature. By increasing the fraction of biodiesel in the blend the discharge coefficient does not change significantly. The viscosity of fuel seems pilot the closing delay and influence the discharge coefficient but for negative temperature it seems not be the alone property to modify the injector performance. In fact with B100 the discharge coefficient tends to be strong lower than that of diesel and biodiesel blended fuels. However By decreasing the temperature of fuel, the discharge coefficient tends to be same for diesel fuel and biodiesel blends. The result for spray behavior shows that spray penetration increases and spray angle strongly decreases. Those behaviors are particularly clear for the B100 fuel. In effect, when the temperature is reduced to a value close to the fuel cloud point, their flow abilities and spray behaviors are worsened.

Introduction

Biodiesel is a very interesting fuel because it is renewable, thus increasing energy security, environmentally friendly, and has a higher cetane number and a lower sulfur and aromatic content. The main disadvantages of biodiesel are its higher viscosity, lower energy content, higher cloud point and pour point, higher nitrogen oxide (NOx) emissions, lower power and high price [1]. However, many countries can produce their own biodiesel and blends with diesel fuel of 2-20% [2,3]. Governments (e.g. the European Union, the U.S.A.) have stipulated that fuel should be blended with biodiesel [3], although consumers are unconvinced about the use of biodiesel fuel blends in automotive engines because of concerns about combustion efficiency, pollutant emissions and the effects on engine components. Attention is especially focused on pollutant emissions from biodiesel fuelled vehicles as in 2014 they have to respect Euro VI regulations.

The new standards include the cold-start problems: evaluation of post-treatment strategies and EGR at low temperature. Quality cold start at 266 K is a benefit that will become increasingly stringent. For these temperatures the viscosity is greater. The blending of biodiesel with diesel fuel causes of the cloud point, the cold filter plugging point (CFPP) pour point or to increase, which can clog the fuel lines and filters of the vehicle's fuel system [4]. Anyway, diesel-biodiesel blends under 5 %, don't impact cold flow properties [27]. That is why it is important to know the behavior of the diesel injector to these conditions for different fuels.

Several publications [4, 5, 6, 7, 8, 9, and 23] have highlighted the influence of fuel properties on the performance of the injector under standard temperature conditions. The increased viscosity decreases slightly in the flow rate in the nozzle and favors the appearance of larger drops in the spray atomization. However, the decrease in the coefficient of discharge is not observed on mixture of biodiesel. It was only out of pure biodiesel [10, 11]. In the other side the literature shows that is not easy to find a relation between the fuel mass flow rate and temperature. It depends on type of injector and type of fuel [12, 13]. These two studies show that, at cold conditions, the discharge coefficient (Cd)

decreases strongly with a viscosity increase [12]. Breda Kegl [14] studied for a specific configuration (a single injection assembly of inline fuel injection system) the impact of temperature on biodiesel. He shows when the temperature decreases the injection duration, injection timing, the mean injection rate and the injection pressure increase. The literature lacks of information on the injection rate of diesel-biodiesel blends fuels under cold conditions. Several studies show that when the percentage of biodiesel is increased, spray tip penetration also increases and the spray angle decreases [4,6,8,16,17]. This is because the increase in viscosity increases the spray SMD and reduces the atomization capacity [9]. According to the literature, biodiesel fuel produced with vegetable or animal oil can be used with diesel injectors. Desantes et al. [6] studied also on biodiesel produced from rapeseed, in which two biodiesel blends (5% and 30%) and pure biodiesel were studied. The results showed that only pure biodiesel has an effect on the spray behavior. Payri et al. [13] observed effect of fuel properties on diesel spray development in extreme cold condition, they reported on cold conditions (255 K) the penetration length are clearly increased.

In the present study, the chosen fuels were diesel fuel, biodiesel (rapeseed biodiesel), and diesel fuel blended with 20%, 50% rapeseed biodiesel. We also test winter Diesel which has the double interest to have the same kinematic viscosity than B20 and the same density than Diesel. The fuel properties were measured at the operating temperature and 281 K, 273 K, 268 K, 265 K (very near of CFPP) of Biofuel). We investigate the effect viscosity or temperature on the fuel injection rate on the cold conditions, the effect of biodiesel and diesel fuel blends on the injection rate e.g. Injection delay, discharge coefficient, fuel mass flow rate, spray delay. In the second part we study the penetration length and spray angle of Winter diesel spray and pure biodiesel spray.

Material and methods

Experimental setup

Two experimental tests rigs have been used: a injection test rig and visualization test rig. For the two experimentations a prototype CRI 3.1 piezoelectric injector of Bosch with three convergent holes of 100 μm of diameter with pump and a pressure fuel tank are used. All injection and visualization equipment were installed in the refrigerator to control the temperature in the experiment. Injection pressures were set at 30-60 MPa to be close of start-up conditions. The fuel injection rate was analyzed according to the Bosch method with an IAV[®] Injection Rate system (model K-025-50). This system detects and processes the dynamic pressure generated by injection into tube loops filled with fuel [15]. The duct is pressurized by an adjusted nitrogen supply until 2.5 MPa showed that Figure 1. The injection rate is computed by equation (1), where \dot{m} is the mass flow rate, S_{tube} the cross sectional area of the tube, a the fuel sound velocity and $p(t)$ the dynamic pressure. The injector is a micro-sac type with three nozzles with conical-shaped orifices. This is same uses in previous studies [9, 10, 13]. The outlet diameter (D_o) of the orifice is 100 μm , and the degree of conicity AR is 38% which limits the cavitation. All injection equipment was installed in the refrigerator to control the temperature in the experiment.

$$\dot{m} = \frac{S_{\text{tube}}}{a} p(t) \quad (1)$$

The macroscopic visualization is made using a constant-volume vessel with optical access and a constant circulation of air near the window showed that Figure 2. To obtain the desired density conditions inside the vessel, the pressure is adjusted and kept constant in function of set point temperature; the system is designed for a maximum pressure of 3 MPa. The fuel injector is located at the top of the vessel. The 8-bit (256 gray levels) high speed camera (Photron[®] PowerViewTM HS-2000) records 15,000 frames per second and captures the three sprays by Mie scattering. Illumination is created with a continuous 150 W halogen lamp. Camera and lamp are outside of climatic chamber, only a fiber light is inside. The image processing is based on Dernet et al. [8] and Tinprabath et al. [11]. For each operating condition, 50 injection sequences were recorded to ensure convergence of the results. For study injection; five fuels were tested: diesel fuel, winter diesel fuel, two diesel-biodiesel blends: B20, B50, and pure biodiesel (B100) and for the spray behavior study; Winter diesel fuel and B100 were used. Injection pressures were set at 30-60 MPa. The experimental temperatures studied were set at room temperature, 268 K and 265 K. On the 265 K is the lowest operating temperature in which a vehicle or cold filter plugging point (CFPP) of biodiesel fuel.

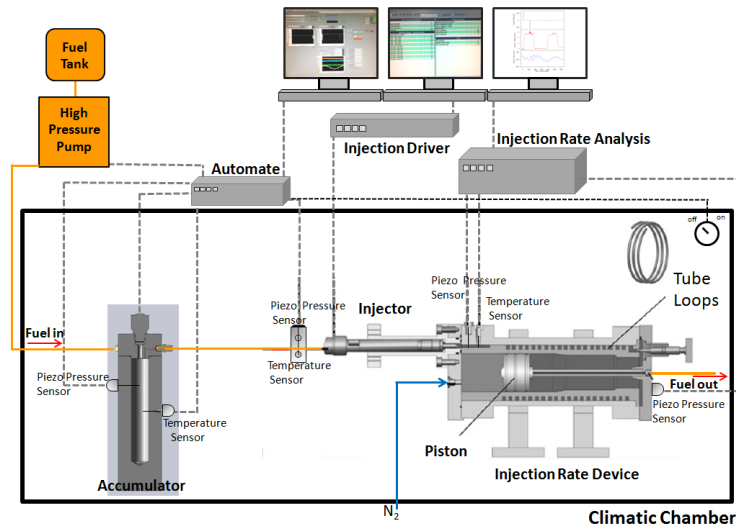


Figure 1. Injection rate experimental setup (from IAV[®] technical specification) [7, 11].

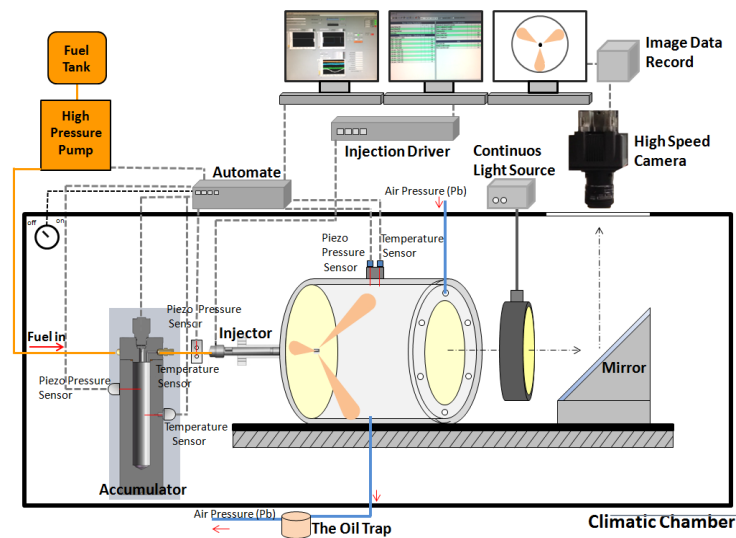


Figure 2. Experimental setup for spray injection.

Spray image analysis

Raw images were analyzed using a digital image processing program to determine the spray tip penetration S and spray angle θ at $S/2$. In summary there are three main steps. First, the background is subtracted from the spray region and then it is converted to a negative image. Second, the image is binarized by applying an intensity threshold level according to the Otsu method [26], to “separate” the spray from the background. Third, from the digitized images, the spray tip penetration S is measured, as well as the spray angle at $S/2$.

Experimental test fuels

The five fuels chosen in this study are Diesel, Winter diesel and a mixes between Diesel and Rapeseed biodiesel. They are referenced in this study as follows: Diesel, Winter diesel, B100 (biodiesel 100 % produced from rapeseed), B20 (diesel 80%, biodiesel 20 and B50 (diesel 50%, biodiesel 50 %). The fuel density and viscosity were analyzed with an Anton Paar[®] Stabinger Viscosmeter (model SVM 3000/G2). The fuel properties are listed in Table 1 and on Figure 3.

Table 1. Density, ρ (kg/m³) and Kinematic viscosity, ν (mm²/s) of fuel at atmospheric pressure.

T(K)	Density, ρ (kg/m ³)					Viscosity, ν (mm ² /s)					
	Diesel	Winter Diesel	B20	B50	B100	Diesel	Winter Diesel	B20	B50	B100	
265	855.1	853.5	863.3	877.4	900.2	10.38	11.43	11.63	15.42	19.72	
268	852.3	851.4	860.6	874.9	897.7	8.95	9.65	10.07	12.64	16.04	
273	848.8	847.4	857.1	871.1	894.1	7.51	8.04	8.24	9.95	13.03	
281	843.2	842.4	851.4	865.5	888.3	5.85	6.19	6.40	7.68	9.97	
293	834.7	834.1	842.9	856.9	879.6	4.23	4.43	4.61	5.49	7.05	

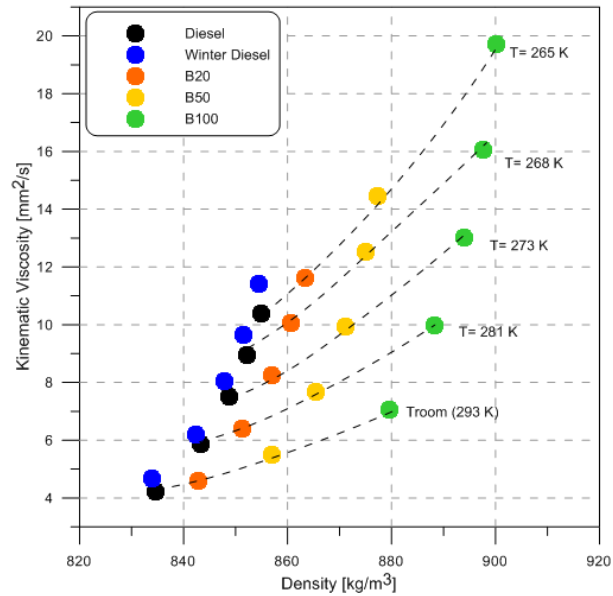


Figure 3. Fuel matrix – predicted viscosity versus predicted density.

We experiment to find density and viscosity, using the correlation from M.R. Riazi [24] for calculate the density and viscosity [Equation (2-5)].

$$\rho_T = 0.99SG - 10^{-3} \cdot (2.34 - 1.898SG) \cdot (T - 288.7) \quad (2)$$

The choice of one set of coefficient is not valuable for all temperature range to describe the evolution of viscosity. We separate the curve in two parts.

For the temperature 270 K to 313 K,

$$\log_{10}(\nu_T) = A \left(\frac{311}{T} \right)^B - a \quad (3)$$

$$A = \log_{10}(\nu_{311(100)}) + a \quad (4)$$

$$B = b \cdot \log_{10}(\nu_{311(100)}) + c \quad (5)$$

The coefficient values a , b , c are obtained by minimizing the sum of square errors between the correlation and experiment: $a = 1.1865$, $b = -0.4144$, $c = 2.0082$.

For the temperature 269 K to 263 K,

$$\text{Log}_{10}(v_T) = A \left(\frac{269}{T} \right)^B - a \quad (6)$$

$$A = \log_{10}(v_{269(100)}) + a \quad (7)$$

$$B = b \cdot \text{Log}_{10}(v_{269(100)}) + c \quad (8)$$

The coefficient values a , b , c are obtained by minimizing the sum of square errors between the correlation and experiment: $a = -0.8639$, $b = -87.6560$, $c = 124.30$. The results from experiment and correlation show in the Figure 4. The star point is the point to separate the impact of viscosity and density. The behaviour of different fuels with the same density of 857 kg/m^3 (+/- 0.5%) and the same viscosity of $10 \text{ mm}^2/\text{s}$ (+/- 4%) are investigate.

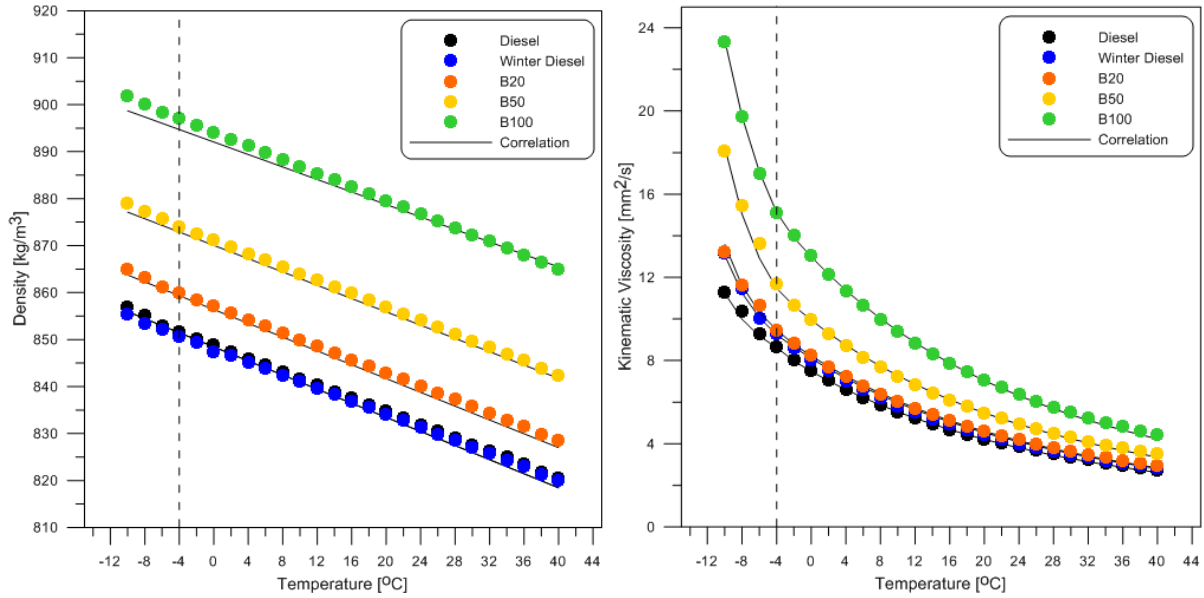


Figure 4. Density and Kinematic viscosity experimental data - correlation.

Operating conditions

The injection rate experiment was carried out at operating temperature and at 281 K, 273 K, 268 K, 265 K. The injection pressure, P_i , varied from 30 – 60 MPa and the back-pressure, $P_b = 2.5 \text{ MPa}$. The duration of electrical activation of the injector was set at $2000 \mu\text{s}$ for effective injection duration of about $4000 \mu\text{s}$. Each injection event was reproduced 50 times. The injection frequency was set at 1 Hz to allow the pressure waves in the injection device and in the duct upstream of the injector to be completely dampened [7, 11]. For each injection the temperature of fuel, the injection pressure is recorded. Temperature stays constant for all injection strokes, with variations +/- 0.3 K. The behavior of injector is very stable after 18 injections. Each injection rate is divided into three parts: opening, quasi steady period and closing. The discharge coefficient (C_d) calculated for each condition corresponding to the mass flow rate was averaged between 1000 and $2000 \mu\text{s}$ after the start of activation (SOA) during the quasi-steady state period (Figure 5).

The spray injection experiment was also conducted at room temperature (293 K), 265 K, 268 K. The injection pressure, P_i varied from 30 and 60 MPa and the back-pressure, P_b at 1.7 MPa for density 20.1 kg/m^3 . The injection duration was set at $2000 \mu\text{s}$ and the injection frequency at 1 Hz.

injection analysis

The injection rate analysis method used followed Payri et al. [9, 18], Dernote et al. [7] and Tinprabath et al. [11] equation (9) was used to calculate the discharge coefficient C_d , by mean mass flow rate, $\dot{m}_{\text{measured}}$ from the quasi-steady state period 1000 - 2000 μs after the start of activation (SOA)(Figure 5). This period avoids the transient phenomena related to the opening and closing phases of the injector [7, 11]. The theoretical mass flow rate (equation (10)) is derived from a combination of the continuity equation (equation (11)) and Bernoulli's equation (equation (12)), assuming that the inlet velocity was negligible:

$$C_d = \frac{\dot{m}_{\text{measured}}}{\dot{m}_{\text{th}}} \quad (9)$$

$$\dot{m}_{\text{th}} = n_{\text{orifice}} \cdot S_c \sqrt{2\Delta P \cdot \rho_f} \quad (10)$$

$$\dot{m}_{\text{th}} = n_{\text{orifice}} \cdot \rho_f \cdot S_c V_{\text{th}} \quad (11)$$

$$V_{\text{th}} = \sqrt{\frac{2\Delta P}{\rho_f}} \quad (12)$$

When n_{orifice} is the number of orifices on the outlet geometric cross-section area of the orifice, ΔP the pressure differential ($\Delta P = \text{injection pressure}(P_i) - \text{back pressure}(P_b)$), ρ_f the fuel density of fuel at experimental temperature, V_{th} the theoretical velocity at the fuel outlet section. Re the Reynolds number is calculated by equation (13), where V_{mean} is the fuel mean velocity at the orifice exit, D_o is the geometric outlet diameter and ν is the kinematic viscosity of the fuel at experimental temperature at atmospheric pressure. V_{mean} , the fuel exit mean velocity (equation (14)) can be determined by measuring mass flow rate and using the continuity equation. For the fuel mean velocity considering, the outlet geometric cross-sectional area (S_c), assumes that there is no area, contraction flow of fuel smaller than the outlet diameter induced by potential cavitations [8,13], flow losses are attributed to losses of flow velocity.

$$Re = \frac{V_{\text{ef}} \cdot D_o}{\nu} \quad (13)$$

$$V_{\text{mean}} = \frac{\dot{m}_{\text{measured}}}{n_{\text{orifice}} \cdot S_c \cdot \rho_f} \quad (14)$$

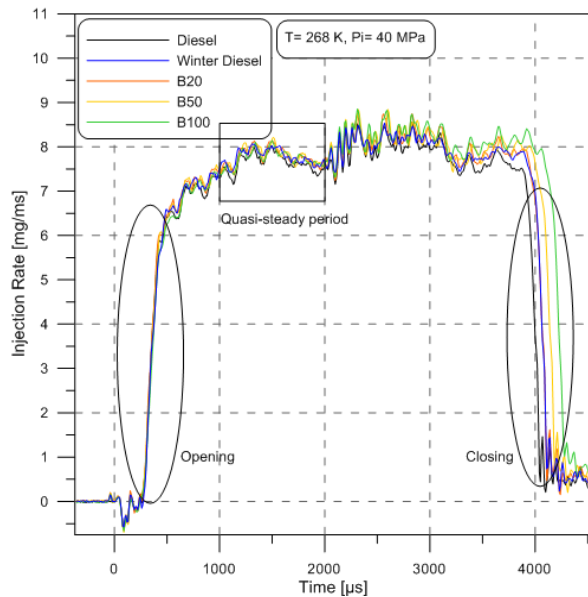


Figure 5. Mean mass flow rate $P_i = 40 \text{ MPa}$, $P_b = 2.5 \text{ MPa}$, $T = 268 \text{ K}$.

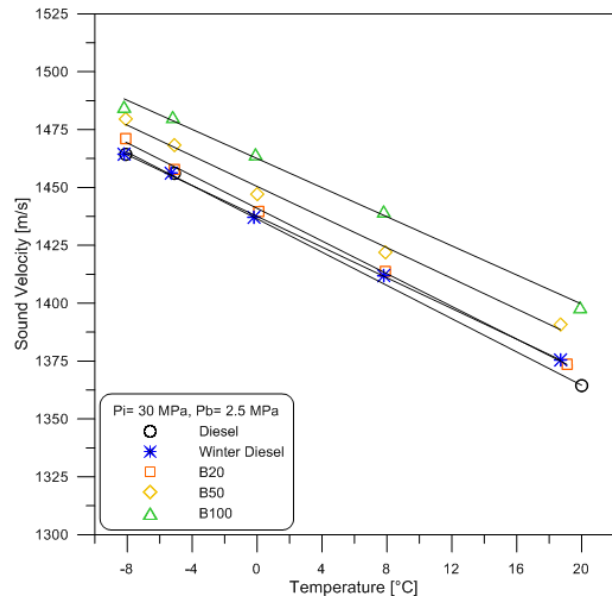


Figure 6. Sound velocity as a function temperature. for fuels tested at $P_b = 2.5 \text{ MPa}$.

Sound velocity measurement

Sound velocity is an important thermophysical property of fuel, as it directly characterizes the fuel injection and NO_x emissions in diesel engines [19]. It is necessary in order to determine the mass flow rate (see equation (1)). The injection rate device can be used to estimate sound velocity [7, 20]. The method is based on determination of the time delay between the incident signal induced by the injection event and the first reflection wave [7]. The distance travelled by the pressure wave is 10.2 m with a maximum error of 0.3%. The acoustic wave is generated by an injection from 30 to 60 MPa in the injection rate system under a back-pressure at 2.5 MPa. In our case (Figure 6), we chose a linear fit to show that the sound velocity increases approximately linearly when the temperature decreases. These experimental values at room temperature are close to the measurements made by Dernotte et al. [7] and Tinprabath et al. [11] and the experimental values at cold temperatures are close to the measurements made by Kegl et al. [20].

Results and Discussion

Effect of cold temperature and blended fuel properties during the opening and closing of injector

With the piezoelectric technology, with a strong activation of needle, the change of fuel or of temperature changes only very little the opening of injector. The delay depends on valve and needle displacement. Figure 7 shows that the mean mass flow rate and variation of pressure upstream of injector for Winter diesel and B100 at $P_i=30$ MPa. The pressure drop is caused by the opening of the valve. The acoustic pressure wave is then disturbs the needle removed, pressure increases and then decreases. With the B100 at low temperature, the pressure decrease is slower, the needle is lifted slightly delayed then explaining the increase of hydraulic delay of 15 μ s. This shift is much more important to closing like observed. However the modification of fuel and temperature has a big impact on closing delay like observed in Figure 5. The delay closing in the fuel of injection increases with the biodiesel content, with the B100 fuel showing the most delayed closing. The needle displacement due of pressure drop inside injector depends on frictional forces so on the viscosity of fuel. B20 and winter diesel with the same viscosity and a different density show the same closing delay. This behavior is typical for this technology. With a solenoid activation, the movement of the needle at higher viscous fluid is more difficult for the opening and the closing of injector [11]. With decrease in temperature the viscosity of fuel increases. So the closing delay increases and leads an increase of injection duration. The results are similar to the findings of Breda Kegl [14].

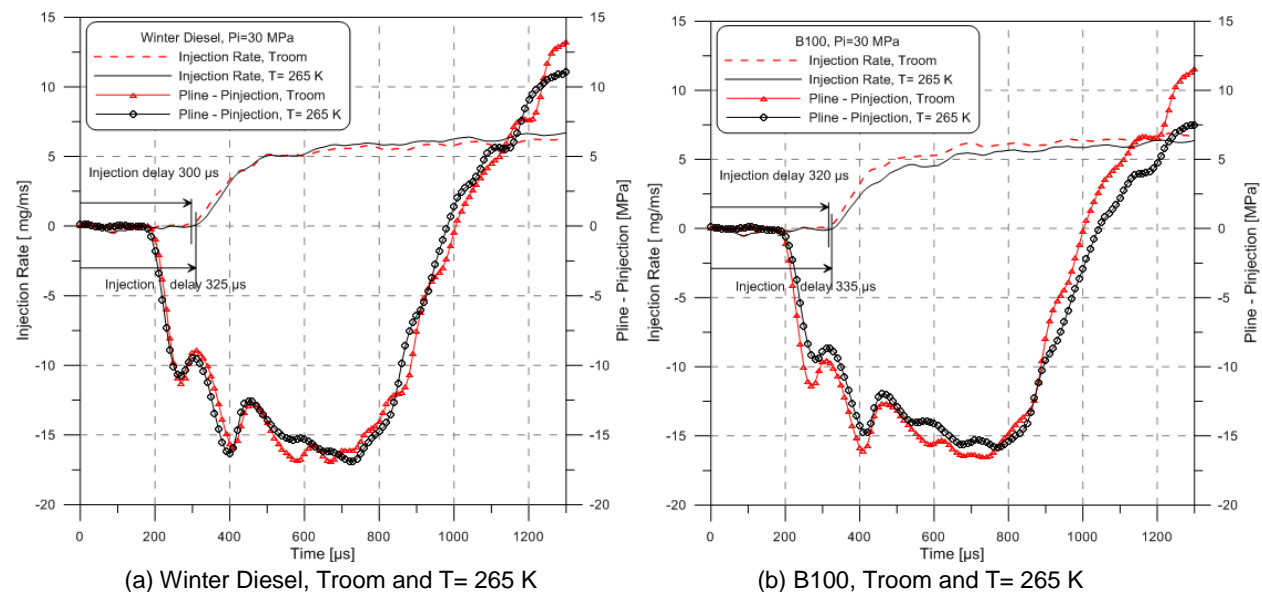


Figure 7. Mean mass flow rate and Pline – Pinjection of Winter diesel and B100 - $P_i=30$ MPa.

Discharge coefficient

We analyze data during the quasi steady period according to equation (9). The Figure 8(a) shows the discharge coefficient versus the pressure difference for different fuels at room temperature. The discharge coefficient has been affected from biodiesel blend or viscosity increasing at room temperature. These decrease is more important for small

injection pressure : 2.6 % for $P_i=30$ MPa and 0.6 % for $P_i=60$ MPa. The results are similar to the findings of Seykens et al. [25], Desantes et al. [6], Park et al. [10] and Tinprabath et al. [11]. This behavior is confirmed until 273 K, on Figure 9(b) the C_d decreases linearly with viscosity at injection pressure 30 MPa. The discharge coefficient of diesel fuel tends to lowest all fuel and maximum the percentage difference is 2.4 %. Likewise, in cold conditions at 265 K it is nearly of CFFP of biodiesel fuel, Figure 9(a) shows the discharge coefficient versus the pressure difference for different fuels at temperature). The results show that the discharge coefficient of Winter Diesel fuel is highest all fuel even if this has the same kinetic viscosity of B20. Does not have a significant difference between the discharge coefficient with Diesel or biodiesel blends was observed in the range of injection pressures used here.

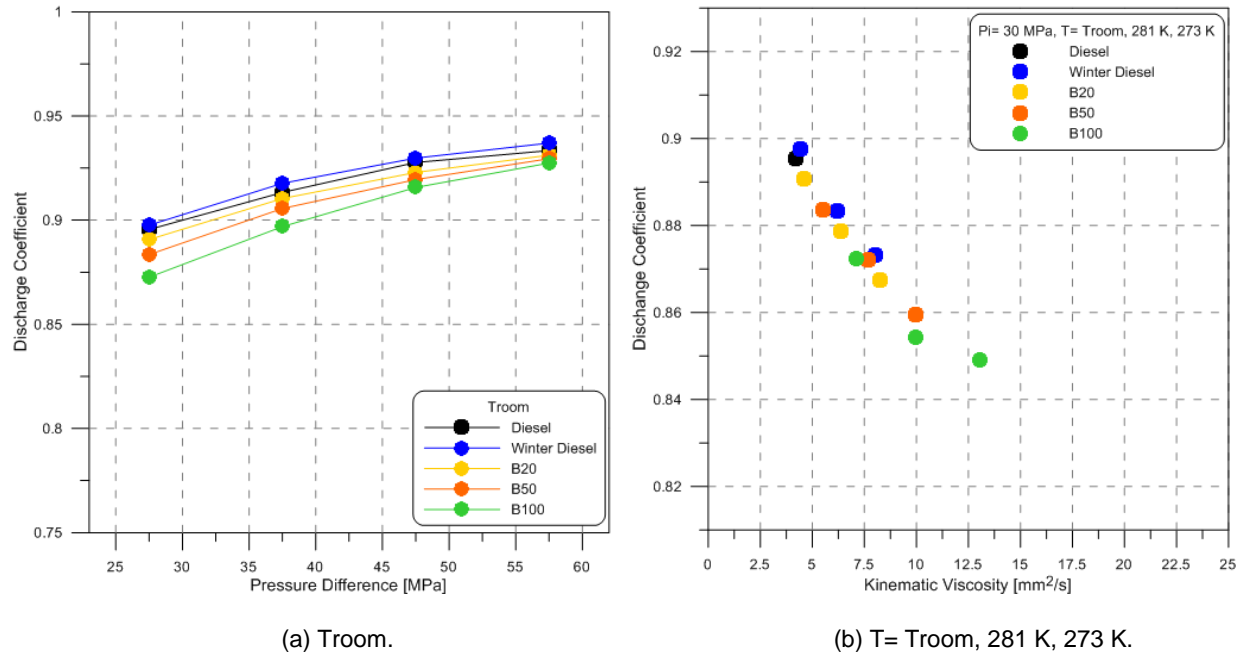


Figure 8. Impact of fuel blends and temperature on the discharge coefficient – $P_i = 30 - 60$ MPa.

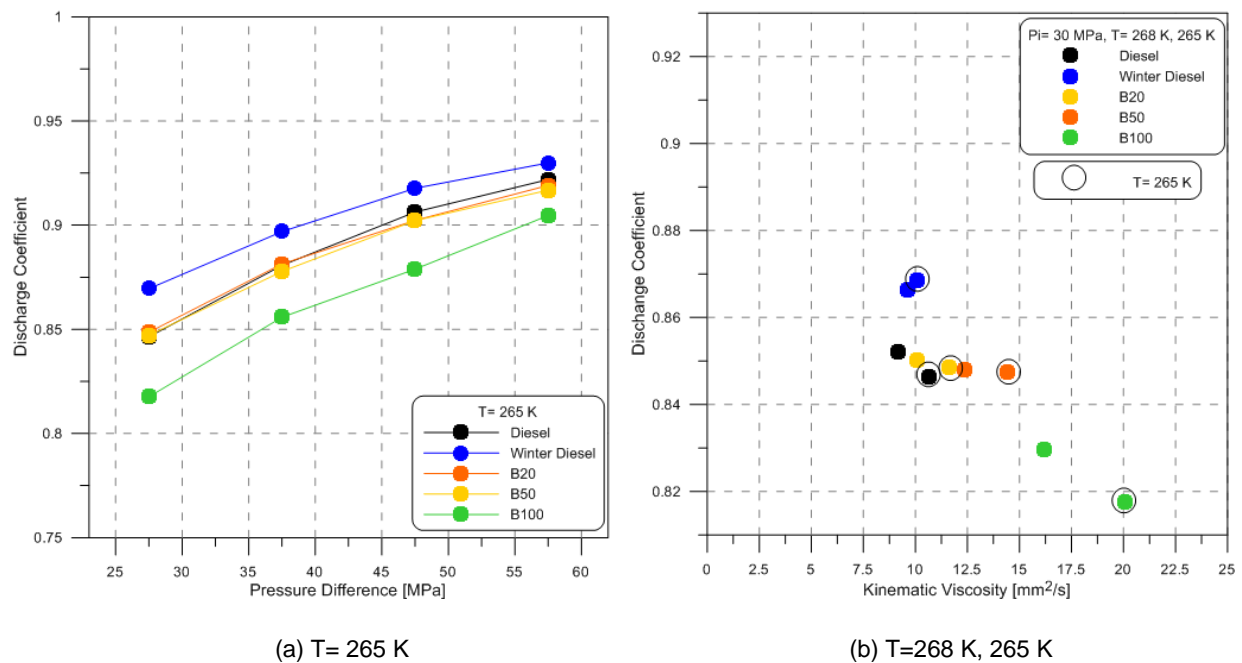


Figure 9. Impact of fuel blends and temperature on the discharge coefficient – $P_i = 30 - 60$ MPa.

However, the discharge coefficient strong decrease was observed with B100. For 268 K and 265 K the Cd for fuel blends is not only determined by viscosity. Figure 9(b), the point are more dispersed, this dispersion can be explained with different points: additives-fuel for winter diesel and Diesel improves the discharges coefficient, the temperature is very low (265 K) near of CPPF of B100.

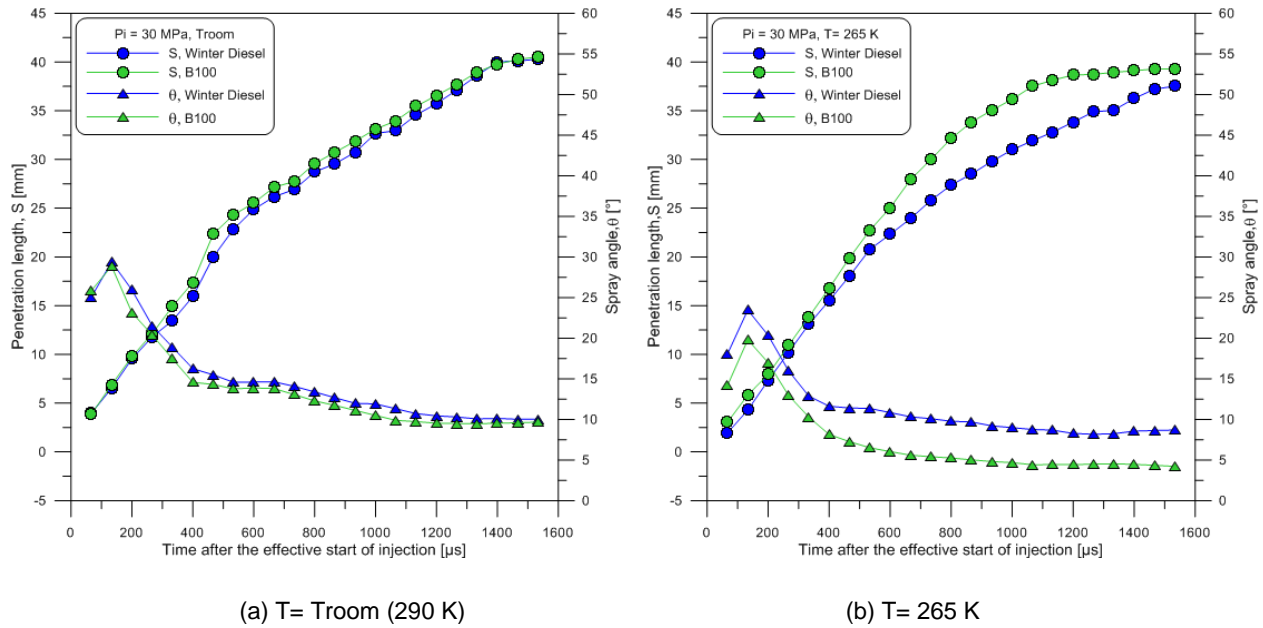


Figure 10. Penetration length and spray angle - $P_i = 30 \text{ MPa}$, $\rho_a = 20.1 \text{ kg/m}^3$.

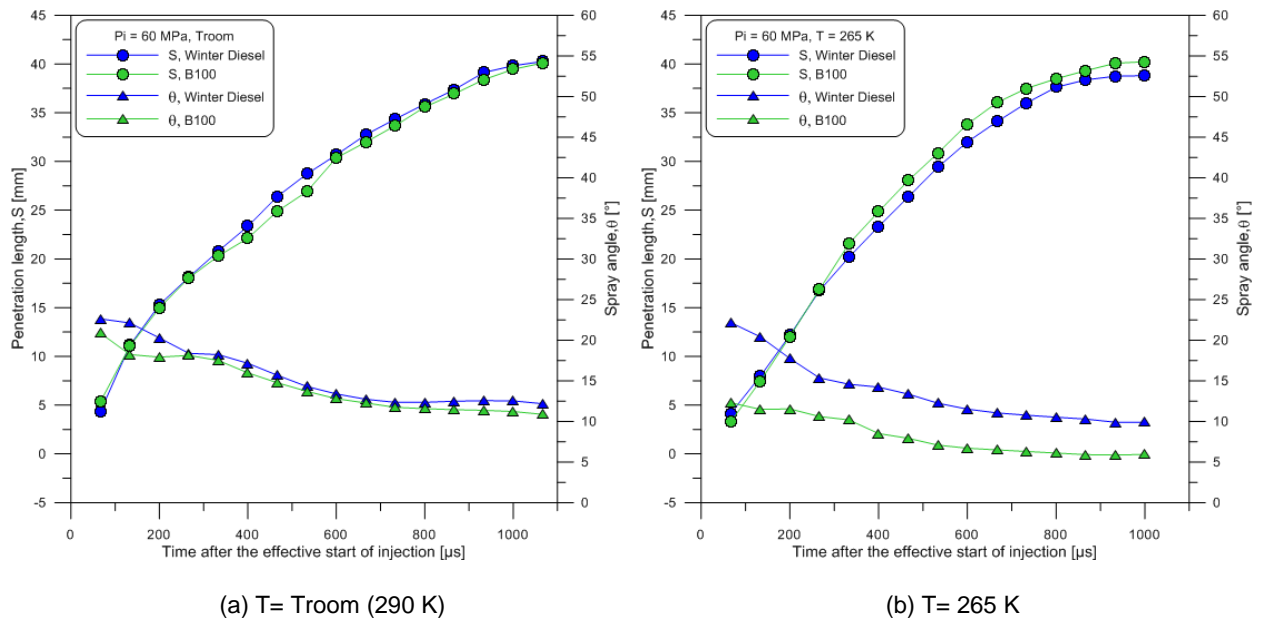


Figure 11. Penetration length and spray angle - $P_i = 60 \text{ MPa}$, $\rho_a = 20.1 \text{ kg/m}^3$.

Penetration length and spray angle

Literature has shown that for ambient temperature, the spray penetration and the angle at the top differ very little from diesel to biodiesel [6,11]. These results are confirmed by our measure (Figure 10(a)). At low temperature the gap is widening (Figure 11(b)). The angle for the B100 is much narrower than the Winter diesel. As expected by Sazhin et al.

[22] spray penetration following two trends first is linear and second depends on square of root of time marking the beginning of the secondary breakup. At the cold conditions 265 K, the penetration length of B100 longer than Winter diesel and spray angle of B100 strong reduce more than Winter diesel. The cold temperature leads to reduce atomization of spray. Spray angle does not only depend on density, it is more sensitive on variation of viscosity (Figure 12). We compare the experimental data with a correlation from Dernotte et al. [8] by equation (15). The spray angle versus viscosity shown in Figure 12, with the same parameter defined by Dernotte et al. the results are agree.

$$\tan\left(\frac{\theta}{2}\right) = A \cdot \left(\frac{\rho_a}{\rho_f}\right)^B \cdot \Delta P^C \cdot f(v) \quad (15)$$

$$\text{Where: } f(v) = e^D \cdot \Delta P^E \cdot v \quad (16)$$

With, $A = 0.24$, $B = 0.24$, $C = 0.08$, $D = -2.4$, $E = -0.58$, v is in mm^2/s , ΔP in MPa.

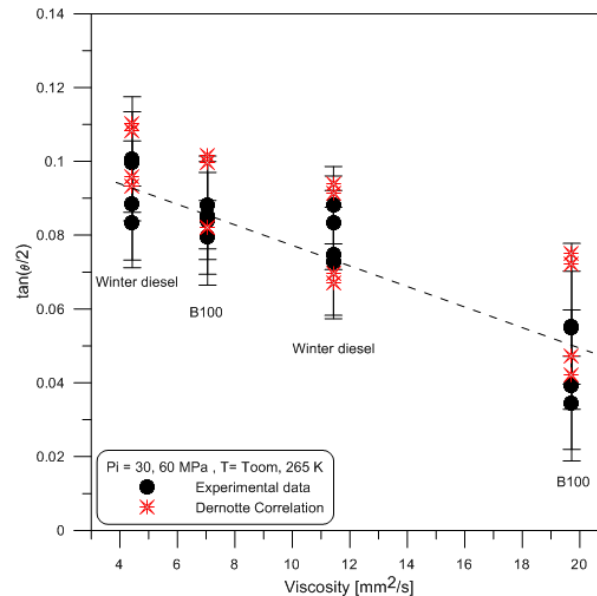


Figure 12. Spray angle versus viscosity - $P_i = 30, 60 \text{ MPa}$.

Conclusions

The study of the influence of biodiesel and diesel blends on the injection rate in cold conditions was conducted using Bosh CRI 3.1 piezoelectric injector. Measurements of the mass flow rate and visualization of spray with diesel fuel, winter diesel fuel, biodiesel blends and Biodiesel (B100) were made.

We make an effort to research and find a new understanding of the injection rate behaviors under cold conditions and focus on low injection pressure. Our results are compared with data available in the literature. The conclusions of this study are summarized as follows:

- For this type of injector, the fuel viscosity changes the injection duration.
- Concerning the performance of the injector shown by the value of the coefficient of discharge, two behaviors are visible: at positive temperatures or for fuels without additives (B100), the discharge coefficient decreases linearly with increasing viscosity; at negative temperatures for fuels with additives (Winter diesel, Diesel or blend), the viscosity is not only a property which modifies the discharge coefficient. The effect of additives cancels the impact of viscosity and the Diesel and Blends fuel are the same discharge coefficient. For Winter diesel with different additives, the discharge coefficients are better.
- The angle of spray is smaller when the temperature decreases or when the viscosity increases. The cold temperature seems to reduce the atomization of spray.

Nomenclature

a	Fuel sound velocity [m/s]
AR	Degree of conicity (area reduction) [-]
C_d	Discharge coefficient [-]
$CFPP$	Cold filter plugging point [K]
CP	Cloud point [K]
D_i	Inlet diameter [m]
D_o	Outlet diameter [m]
\dot{m}	Mass flow rate [mg/ms]
\dot{m}_e	Estimated mass flow rate [mg/ms]
$\dot{m}_{measured}$	Mean mass flow rate [mg/ms]
\dot{m}_{th}	Theoretical mass flow rate [mg/ms]
$n_{orifice}$	Number of orifices on the nozzle [-]
P_b	Back-pressure [MPa]
P_i	Injection pressure [MPa]
PP	Pour point [K]
$p(t)$	Dynamic pressure [MPa]
ΔP	Pressure difference [MPa]
Re	Reynolds number [-]
S	Spray penetration length [mm]
S_c	Outlet geometric cross-sectional area [m ²]
SG	Specific gravity @ 288.5 K [-]
S_{tube}	Cross-sectional area of the measuring tube [m ²]
V_{mean}	Mean velocity at the outlet section [m/s]
t	Time [μ s]
T	Fuel temperature [K]
T_{room}	Room temperature [K]
ν	Fuel kinematic viscosity [mm ² /s]
$\nu_{311(100)}$	Fuel kinematic viscosity at $T = 311$ K [mm ² /s]
$\nu_{269(100)}$	Fuel kinematic viscosity at $T = 269$ K [mm ² /s]
ρ	Fuel density [kg/m ³]

References

- [1] Demirbas, A., 2009, Energy Conversion and Management, 50, pp. 14-34.
- [2] No, S.Y., 2011, Atomization and Spray, 21(1), pp. 87-105.
- [3] Perdiguero, J., and Jimenez, J.L., 2011, Renewable and Sustainable Energy Reviews, 15, pp.1525-1532.
- [4] Bang, S.H., and Lee, C.S., 2010, Fuel, 89, pp. 797-800.
- [5] Som, S., Longman D.E., Ramirez, A.I., and Aggarwal, S.K., 2010, Fuel, 89, pp. 4014-4024.
- [6] Desantes, J.M., Payri, R., Garcia, A., and Manin, J., 2009, Energy & Fuels, 23, pp. 3227-3235.
- [7] Dernet, J., Hespel, C., Foucher, F., and Mounaïm-Rousselle, C., 2012, Fuel, 96, pp. 153-160.
- [8] Dernet, J., Hespel, C., Foucher, F., and Mounaïm-Rousselle, C., 2012, Atomization and Spray, 22(6), pp. 461-492.
- [9] Payri, R., Salvador, F.J., Gimeno, J., and Morena, J., 2009, Fuel, 30, pp. 768-777.
- [10] Park, S.H., H.K., and Lee, C.S., 2008, Energy & Fuels, 22, pp. 605-613.
- [11] Tinprabath, P., Hespel, C., Chanchona, S., and Foucher, F., 2013, SAE Tech paper, 240032.
- [12] Vergnes, C., Foucher, F., and Mounaïm-Rousselle, C., 2009, Atomization and sprays, 19(7), pp. 621-631.
- [13] Payri, R., Salvador, F.J., Gimeno, J., and Brach, G., 2008, Automobile Engineering, IMechE Vol.222 Part D J, pp. 1743-1753.
- [14] Kegl, B., 2008, Fuel, 87, pp. 1306-1317.
- [15] Bosch, W., 1996, SAE Technical paper, 660749.
- [16] Gao, Y., Deng J., Li, C., Deng F., Liao, Z., Wu, Z., and Li, L., 2009, Biotechnology Advances, 27, pp.616-624.
- [17] Chen, P.C., Wang, W.C., Roberts, W.L., and Fang, T. Fuel, 2012;103:850-861.
- [18] Payri, P., Garcia, J.M., Salvador, F.J., and Gimeno, J., 2005, Fuel, 84, pp.551-561.
- [19] Freitas, S. V.D., Paredes, Maecio, L.L., Daridon, J.L., Lima, A.S., and Coutinho, Joao, A.P., 2012, Fuel, 103, pp. 1018-1022.
- [20] Kegl, B., and Hribernik, A., 2006, Energy & Fuels, 20, pp. 2239-2248.
- [21] Naber, J.D., and Siebers, D.L., 1996, SAE Technical paper 960034.
- [22] Sazhin, S.S., Feng, G., and Heikal, M.R., 2001, Fuel, 80, pp. 2171-2180.

- [23] Sarin, A., 2012, "Biodiesel production and properties".
- [24] Riazi, M.R., 2005, "Characterization and properties of petroleum fractions".
- [25] Seykens, X.L.J., Somers, L.M.T., and Baert, R.S.G., July. 6.-9. 2004. In: Proceedings of VAFSEP.
- [26] Otsu N., IEEE Trans. Syst. Man Cyber, 1979, vol. 1: 62-66.
- [27] National Biodiesel Board, <http://www.biodiesel.org> ([cit. 2014-03-20]).